Physical human-robot interaction with a backdrivable (6+3)-dof parallel mechanism

Louis-Thomas Schreiber[1] and Clément Gosselin[2]

Abstract— **This paper presents a kinematically redundant spatial parallel mechanism with 3 redundant dofs and how it can be used for physical human-robot interaction. The architecture of the mechanism is similar to the well-known Gough-Stewart platform and it retains its advantages, i.e., the members connecting the base to the moving platform are only subjected to tensile/compressive loads. The kinematic redundancy is exploited to avoid singularities and extend the rotational workspace which is very important in the context of haptic devices. The architecture is described and the associated kinematic relationships are presented. Solutions for the inverse and direct kinematics are given, as well as a simple gravity compensation model. Finally, a control scheme enabling physical human-robot interaction while controlling the 3 redundant degrees of freedom is given.**

I. INTRODUCTION

Despite being widely used in the flight simulation industry (see for instance [1]), precision mechanisms (see [2]) and pick and place tasks (see [3]), parallel robots still represent a very small portion of the world total robot population [1]. Indeed, parallel robots lack the large workspace required in most assembly and welding applications. Another field in which parallel robots are commonly used is haptic interface. Generally coupled with a serial mechanism for the orientation, parallel mechanisms are widely used in haptic interface (such as the ones used to control surgical robot) because of their high transparency. Indeed, their high stiffness/inertia ratio is excellent compared to serial mechanisms. Their main drawback remains their limited workspace though, which explains why serial wrist are generally for the orientation.

The subject of workspace improvement of parallel robots is not new (see [4], [5], [6], [7]), especially for the Gough-Stewart platform (GS platform). However, although significant efforts were deployed, the GS platform's workspace is still very limited by the so-called type II (or parallel) singularities [8]. The determination of the geometric conditions that lead to such singularities and the characterization of the locus of these singularities in the workspace has been the subject of several research studies (see [4], [5], [9] for example). Notwithstanding the above efforts, the GS platform has seen very few changes since its introduction in 1954 [10], [11] and its orientational workspace is limited to relatively small rotations. In most cases, the maximum tilt angle that a platform can reach is approximately 45^o.

Some researchers are nevertheless working on means of expanding the workspace of parallel robots and some promising solutions have been proposed. One solution, among others, is to include kinematic redundancy (see [12] for a complete review of redundancy in parallel mechanisms). It was shown in [13], [14] that this principle can completely remove singularities from the workspace of some parallel robots while still being simple to implement. It was also shown in [15] that kinematic redundancy can be introduced in the GS platform using an architecture that preserves the force transmission properties while avoiding actuation redundancy in order to improve the rotational workspace. In this reference, it was shown that 3 redundant dofs are theoretically sufficient to avoid all singularities. Determining the ideal configuration is relatively simple with one redundant dof (see [13], [14] for examples with planar mechanisms), but it can be more challenging when the number of redundant dofs increases.

This paper explains how a (6+3)-dof parallel mechanism can be used in physical human-robot interaction.

This paper is structured as follows. The architecture of the redundant mechanism (which includes 3 redundant legs and 3 non-redundant legs) is first described. Then, the kinematic modelling is developed. The velocity equations are obtained and the Jacobian matrices associated with the mechanism are derived. The solution of the inverse and direct kinematic problem are given and an index of the force transmission properties of the mechanism is introduced. A simple gravity compensation model developed and, finally, a control scheme enabling physical human-robot interaction while controlling the 3 redundant degrees of freedom is given.

II. MANIPULATOR ARCHITECTURE

The architecture is based on the GS platform, a moving platform connected to a fixed base via six legs of the H$\underline{P}$S type, where H stands for a Hooke (universal) joint, $\underline{P}$ stands for an actuated prismatic joint and S stands for a spherical joint.

The redundant leg used in the architecture proposed in [15] is shown in Fig. 1. The leg comprises two actuated prismatic joints, which are connected to the base via Hooke joints. The prismatic actuators are joined at their tip by a passive revolute joint which connects the two prismatic legs to a link that is in turn connected to the moving platform through a spherical joint.

*This work was not supported by any organization

[1]Département de génie mécanique, Université Laval, 1065 Avenue de la Médecine, Québec, Qc, G1V 0A6, Canada, louis-thomas.schreiber.1@ulaval.ca

[2]Département de génie mécanique, Université Laval, 1065 Avenue de la Médecine, Québec, Qc, G1V 0A6, Canada, gosselin@gmc.ulaval.ca

[1]2943 parallel robots were sold in 2013 compared to 18100 scara robots and 178132 total according to the International Federation of Robotics.

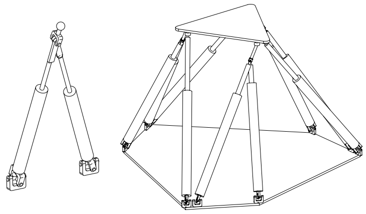

Fig. 1: Architecture of the redundant leg (left) and complete nine-actuator kinematically redundant parallel mechanism (right) (from [15]).

For a given pose of the platform, the two actuated prismatic joints can be driven independently, which allows to orient the link connecting the tip of the prismatic legs to the platform. Moreover, the orientation of this link corresponds to the orientation of the force vector applied to the platform, which determines the Jacobian matrix and the singular configurations. Hence, using the kinematic redundancy of the leg to reorient the link connected to the platform, it is possible to directly affect the Jacobian matrix and avoid singularities, as it was shown in [15]. It is pointed out that all links connecting the fixed base to the platform are subjected to only tensile/compressive loads and since the redundancy introduced in the mechanism is kinematic, there is no actuation redundancy and no antagonistic loads can be generated on the platform by the legs.

A simplified representation of the mechanism is shown in Fig. 1, where three of the legs of a 3–3 GS platform have been replaced with the kinematically redundant legs described above, leading to a mechanism with nine actuators and nine degrees of freedom. Other implementations are also possible.

III. Kinematic modelling

Referring to Fig. 2, a fixed reference frame $Oxyz$ is defined on the base and a moving reference frame $Px'y'z'$ is defined on the platform. The position vector of the centre of the Hooke joints (Universal joints) attached to the base, points A_{ij} or A_i, is noted $\mathbf{a}_i$ for the non-redundant legs and respectively $\mathbf{a}_{i1}$ and $\mathbf{a}_{i2}$ for redundant legs. Similarly, the position vector of the centre of the spherical joint connecting the ith leg to the platform, point B_i, is noted $\mathbf{b}_i$. For redundant legs, the position vector of the centre of the revolute joint connecting the two sub-legs, point S_i, is noted $\mathbf{s}_i$. The length of the link connecting point S_i to point B_i is noted ℓ_i. Finally, the extension of the ith leg is noted ρ_i for a non-redundant leg while the extension of the sublegs are noted ρ_{i1} and ρ_{i2} for a redundant leg.

The Cartesian coordinates of the moving platform are given by the position vector of the reference point P on the platform, noted $\mathbf{p}$, and the orientation of the platform, given by matrix $\mathbf{Q}$, which represents the rotation from the fixed reference frame $Oxyz$ to the moving reference frame $Px'y'z'$. The position vector of point B_i can then be written as

$$\mathbf{b}_i = \mathbf{p} + \mathbf{Q}\mathbf{v}_{i0} = \mathbf{p} + \mathbf{v}_i, \quad i = 1, \ldots, 6 \tag{1}$$

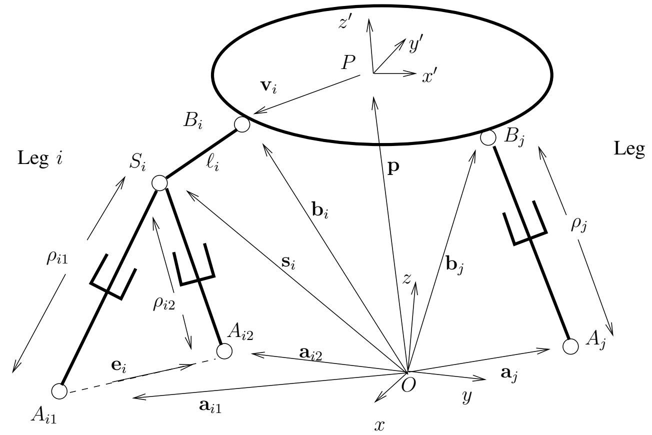

Fig. 2: Kinematic modelling of the mechanism: only one redundant leg and one non-redundant leg are shown.

where $\mathbf{v}_{i0}$ is the position vector of point B_i with respect to point P, expressed in the reference frame $Px'y'z'$. For a given mechanism, this vector is constant. This vector, connecting point P to point B_i, is noted $\mathbf{v}_i$ when expressed in the fixed reference frame.

A. Constraint equations

The derivation of the velocity equations for the non-redundant H$\underline{\text{P}}$S legs is straightforward (see for instance [16]). Indeed, the constraint on the leg lengths can be written as

$$(\mathbf{b}_i - \mathbf{a}_i)^T(\mathbf{b}_i - \mathbf{a}_i) = \rho_i^2. \tag{2}$$

For the redundant legs, referring to Fig. 2, the constraint corresponding to the length of the link connecting point B_i to point S_i can be written as

$$(\mathbf{s}_i - \mathbf{b}_i)^T(\mathbf{s}_i - \mathbf{b}_i) = \ell_i^2 \tag{3}$$

Similarly, the constraint corresponding to the length of each of the sublegs can be written as

$$(\mathbf{s}_i - \mathbf{a}_{ij})^T(\mathbf{s}_i - \mathbf{a}_{ij}) = \rho_{ij}^2, \quad j = 1, 2 \tag{4}$$

where ρ_{i1} and ρ_{i2} are the joint coordinates associated with the two sublegs of the ith redundant leg. Additionally, since the two sublegs are connected with a revolute joint located at point S_i and whose axis is orthogonal to the plane defined by the sublegs, namely the plane defined by points A_{i1}, A_{i2}, S_i and B_i, vectors $(\mathbf{b}_i - \mathbf{a}_{i1})$, $\mathbf{e}_i$ and $(\mathbf{s}_i - \mathbf{a}_{i1})$ must be coplanar. This condition can be expressed as

$$[(\mathbf{b}_i - \mathbf{a}_{i1}) \times \mathbf{e}_i]^T(\mathbf{s}_i - \mathbf{a}_{i1}) = 0, \tag{5}$$

where $\mathbf{e}_i$ is a unit vector passing through point A_{i1} and pointing in the direction of point A_{i2}.

These constraint equations are easily differentiated with respect to time in order to obtain the velocity equations of the mechanism. The complete derivation is presented in [15].

IV. Inverse kinematics

The inverse kinematics is used to find the actuator coordinates from the Cartesian configuration of the platform. This problem is generally straightforward in the case of parallel manipulators since the computation of each actuator coordinate is independent from the other actuated joint coordinates. However for the proposed robot, because of the redundant dofs, there are infinitely many solutions to the inverse kinematic problem. This problem is akin to the inverse kinematics of redundant serial manipulators (see [17], [18]). The configuration of the redundant dofs must be chosen carefully in order to avoid singular configurations. These dofs are determined by the array $\boldsymbol{\gamma}$ containing the angles $\gamma_i, \quad i = 1, 2, 3$. The angle γ_i is the angle that the redundant link $(B_i S_i)$ is making relative to vector $\mathbf{e}_i$, as shown in Fig. 3.

Methods using the velocity equations, similar to the ones used in redundant serial manipulators, can be used also for kinematically redundant parallel manipulators (see [15]). Another option is to consider the redundant dofs as part of the Cartesian coordinates. Determining $\boldsymbol{\gamma}$ is then part of the trajectory planning and the inverse kinematic problem itself becomes simpler. Indeed, with the extended Cartesian coordinates defined as $\mathbf{p}, \mathbf{Q}, \boldsymbol{\gamma}$, it is simple to calculate the position of points B_i using eq. 1. Referring to Fig. 3, the

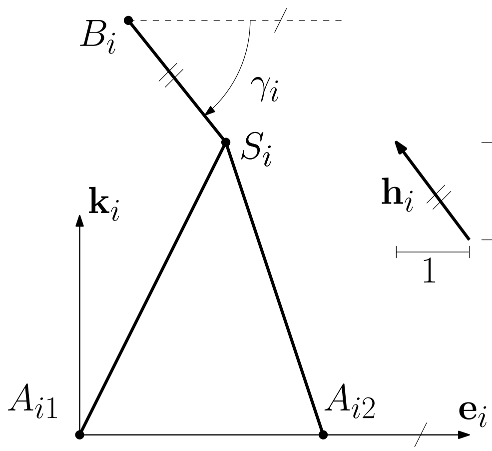

Fig. 3: Geometric representation of a redundant leg.

position vector of point S_i can then be expressed as

$$\mathbf{s}_i = \mathbf{b}_i + \ell \cos \gamma_i \mathbf{e}_i - \ell \sin \gamma_i \mathbf{k}_i \tag{6}$$

where vector $\mathbf{k}_i = \mathbf{g}_i \times \mathbf{e}_i$ and vector $\mathbf{g}_i$ is a unit vector normal to the plane of the redundant leg. Finally, with eqs. 2 and 4, the actuated joint coordinates can be found and there is no need to use the velocity equations to solve the inverse kinematics.

Nonetheless, it is of interest to express the relationship between the time derivative of the extended Cartesian coordinate vector defined as $\mathbf{t}_e = \begin{bmatrix} \dot{\mathbf{p}} & \boldsymbol{\omega} & \dot{\boldsymbol{\gamma}} \end{bmatrix}^T$ and the actuator velocities. This relationship can be expressed as

$$\mathbf{J}_e \mathbf{t}_e = \mathbf{K}_e \dot{\boldsymbol{\rho}} \tag{7}$$

which defines the extended Jacobian matrices of dimension 9×9, $\mathbf{J}_\mathrm{e}$ and $\mathbf{K}_\mathrm{e}$. In order to obtain these matrices, the constraint equation of each actuator of the ith redundant leg (eq. 4) as well as eq. 6 are differentiated with respect to time

$$(\mathbf{s}_i - \mathbf{a}_{ij})^T \dot{\mathbf{s}}_i = \rho_{ij} \dot{\rho}_{ij}, \quad j = 1, 2. \tag{8}$$

$$\dot{\mathbf{s}}_i = \dot{\mathbf{b}}_i - (\ell \sin \gamma_i \mathbf{E}_i - \ell \cos \gamma_i \mathbf{k}_i)\, \dot{\gamma}_i - \ell \sin \gamma_i \dot{\mathbf{k}}_i. \tag{9}$$

Substituting eq. 9 into eq. 8, after some simplifications, yields to matrix $\mathbf{J}_e$

$$\mathbf{J}_e = \begin{bmatrix} \mathbf{c}_{11}^T & [\mathbf{c}_{11} \times \mathbf{v}_1]^T & j_{e,11} & 0 & 0 \\ \mathbf{c}_{12}^T & [\mathbf{c}_{12} \times \mathbf{v}_1]^T & j_{e,12} & 0 & 0 \\ \mathbf{c}_{21}^T & [\mathbf{c}_{21} \times \mathbf{v}_2]^T & 0 & j_{e,21} & 0 \\ \mathbf{c}_{22}^T & [\mathbf{c}_{22} \times \mathbf{v}_2]^T & 0 & j_{e,22} & 0 \\ \mathbf{c}_{31}^T & [\mathbf{c}_{31} \times \mathbf{v}_3]^T & 0 & 0 & j_{e,31} \\ \mathbf{c}_{32}^T & [\mathbf{c}_{32} \times \mathbf{v}_3]^T & 0 & 0 & j_{e,32} \\ \mathbf{u}_4^T & [\mathbf{u}_4 \times \mathbf{v}_4]^T & 0 & 0 & 0 \\ \mathbf{u}_5^T & [\mathbf{u}_5 \times \mathbf{v}_5]^T & 0 & 0 & 0 \\ \mathbf{u}_6^T & [\mathbf{u}_6 \times \mathbf{v}_6]^T & 0 & 0 & 0 \end{bmatrix} \tag{10}$$

. Finally, matrix can be expressed as

where $j_{e,ij} = \|[\mathbf{u}_i \times \mathbf{c}_{ij}]^T\|$, vector $\mathbf{c}_{ij}$ is defined along the subleg j of the redundant leg i, yielding to $\mathbf{c}_{ij} = \mathbf{s}_i - \mathbf{a}_{ij}$ and matrix $\mathbf{K}_e$ is a diagonal matrix containing the joint coordinates, namely $\mathbf{K}_e = diag(\boldsymbol{\rho})$.

V. Direct kinematics

The direct kinematics is used to find the Cartesian configuration $\mathbf{c}$ of the robot from the articular coordinates $\boldsymbol{\rho}$. Solving the constraint equations for $\mathbf{c}$ would lead to very complex equations a high number of equations. The standard Gough-Stewart platform is known to have 40 solution in its direct kinematics. Since the current architecture as 3 suplementary dofs, its direct kinematics is exponentially more complex. Howerver, it is also possible to solve the direct kinematics using a numeric algorythm. This procedure is standard for the direct kinematics of parralel manipulators and for the inverse kinematics of non-decoupled serial manipulators. The algorythm is based on the Newton-Gauss method and is presented in algorythm 1.

VI. Force transmission capabilities

The array of actuator forces $(\mathbf{f})$ generated by a given Cartesian wrench $(\boldsymbol{w})$ is evaluated using the Jacobian matrices as

$$\mathbf{f} = \mathbf{K}^T \mathbf{J}^{-T} \boldsymbol{w} \tag{11}$$

$$\mathbf{F} = \mathbf{K}^T \mathbf{J}^{-T} \tag{12}$$

where $\boldsymbol{w}$ consists of the 6-dimensional vector of forces and moments at the platform. Equation 12 defines the force transmission matrix $(\mathbf{F})$ of the mechanism which can be divided into two separate matrices, one applied to the forces and one to the moments $(\mathbf{F} = [\mathbf{F}_t \quad \mathbf{F}_r])$. In order to obtain the maximal actuator force generated by any combination of Cartesian force and moment unit vectors, the norm of each

Result: $\mathbf{c}_n$
n=1;
$\mathbf{c}_n = \mathbf{p}_n, \mathbf{Q}_n, \gamma_n$ (initial estimation of Cartesian coordinates;
while $\delta \boldsymbol{c}_n < crit$ & $n < n_{max}$ **do**
$\boldsymbol{\rho}_n = \mathrm{IK}(\mathbf{c}_n)$ (find articular coordinates corresponding to estimated Cartesian configuration);
$\delta\boldsymbol{\rho}_n = \boldsymbol{\rho}_m - \boldsymbol{\rho}_n$ where $\boldsymbol{\rho}_m$ is the measured articular coordinates. (Find the error in articular coordinates) ;
$\delta \boldsymbol{c}_n = \mathbf{J}^{-1}\mathbf{K}\delta\boldsymbol{\rho}_n$ (find the Cartesian coordinates adjustment to reduce the error);
$\mathbf{p}_{n+1} = \mathbf{p}_n + \delta\mathbf{p}_n$ (evaluate the new Cartesian coordinates);
$\gamma_{n+1} = \gamma_n + \delta\gamma_n$;
$\mathbf{Q}_{n+1} = \mathbf{R}_x(\delta\theta_x)\mathbf{R}_y(\delta\theta_y)\mathbf{R}_z(\delta\theta_z)\mathbf{Q}_n$;
n=n+1;
end

Algorithm 1: Solving the direct kinematics using a Newton-Gauss method

line of matrices $\mathbf{F}_t$ and $\mathbf{F}_r$ must be combined and then the maximal actuator force can be selected, namely

$$\kappa = max\left(\sqrt{\sum_{j=1}^{3} f_{t,i\,j}^2} + c_r\sqrt{\sum_{j=1}^{3} f_{r,i\,j}^2}, \quad i = 1..9\right) \tag{13}$$

where $f_{x,i\,j}$ is the ith, jth element of matrix $\mathbf{F}_x$.

A weighting between the forces and the moments must be applied since they do not bear the same units and since the maximal Cartesian force value is different from the maximal Cartesian moment value. The weighting between the forces and moments should depend on the actual external forces and moments of a specific application. A generic weighting is therefore difficult to determine. In applications with only gravity and inertial payloads, the distance between the centre of mass of the effector and the reference point P can be used. In applications like machine tools, the distance between the end of the tool and the reference point P can be used. For more insight on the characteristic length of manipulators, see [19] and for more references about manipulator performance indices, see [20], [21], [22]. The results presented in this paper use a value of $c_r = 0.09$m. It corresponds to the assumed distance between the centre of mass of the platform and the reference point P. Additionally, the force transmission index results are scaled by a factor 1.45 in order to obtain a unit value in the reference configuration of the mechanism. Doing this, it is easy to compare the results along the trajectory with the results of the reference configuration.

The maximal admissible value of the force index depends on the ratio of actuator maximal force relative to the maximal payload of the mechanism. Depending on the application, a safety factor and the dynamic loading should be considered. For this paper, no specific application and design are selected. Therefore, a payload of 5 kg and actuators capable of producing 285 N are arbitrarily chosen. These characteristics fit the small dimensions of the mechanism described in section **??**. The corresponding maximal force index is therefore equal to $285/(5*9.81) \approx 5.8$ and once scaled by 1.45, becomes ≈ 4.

VII. Static Model

In order to compensate for gravity in the control loop, a model of the statics forces is necessary. This model can be obtained by expressing the position of the center of mass of every rigid bodies in the mechanism. Because of the parallel architecture, it is more convenient to express the potential energy ($\mathbf{V}$) relative to the Cartesian coordinates. The total potential energy is the sum of all the masses (M_i) times the gravity (g) and their z coordinates relative to the base frame (z_i).

$$\mathbf{V} = \sum_{i=1}^{n} m_i g z_i \tag{14}$$

Refering to Fig. 4, it is simple to express the position of all the center of mass of the rigid bodies ($\mathbf{m}_i$) with the Cartesian coordinates.

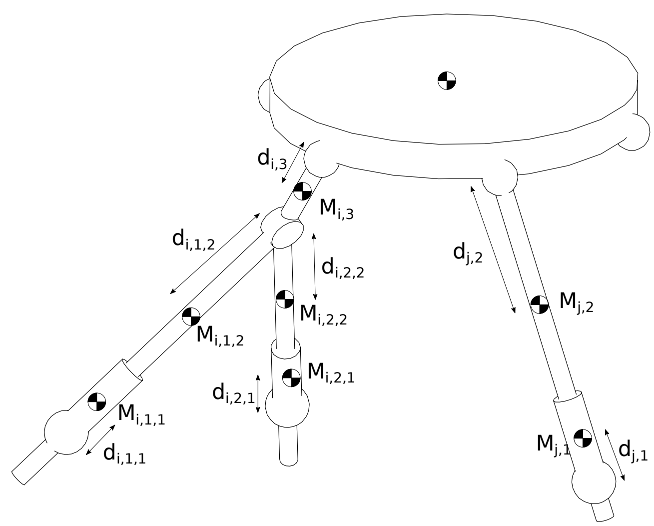

Fig. 4: Parameters of the static model.

$$\mathbf{m}_{i,j,1} = \mathbf{a}_{ij} + d_{i,j,1}\frac{\mathbf{c}_{i,j}}{\parallel \mathbf{c}_{i,j} \parallel} \tag{15}$$

$$\mathbf{m}_{i,j,2} = \mathbf{s}_i - d_{i,j,2}\frac{\mathbf{c}_{i,j}}{\parallel \mathbf{c}_{i,j} \parallel} \tag{16}$$

$$\mathbf{m}_{i,3} = \mathbf{b}_i - d_{j,2}\frac{(\mathbf{s}_i - \mathbf{b}_i)}{\parallel (\mathbf{s}_i - \mathbf{b}_i) \parallel} \tag{17}$$

$$\mathbf{m}_{j,1} = \mathbf{a}_j - d_{j,1}\frac{\mathbf{u}_j}{\parallel \mathbf{u}_j \parallel} \tag{18}$$

$$\mathbf{m}_{j,2} = \mathbf{b}_j - d_{j,2}\frac{\mathbf{u}_j}{\parallel \mathbf{u}_j \parallel} \tag{19}$$

Inserting eqs.(1) and (6) into eqs. (15 - 19), and then using eq.(14), a expresssion of the type

$$\mathbf{K}_p = f(\mathbf{p}, \mathbf{Q}, \boldsymbol{\gamma}) \tag{20}$$

is obtained. This expression can easily be differentiated with respect to the Cartesian coordinates to obtain the resultant equivalent Cartesian wrench $\boldsymbol{w}_g$ generated by gravity, as stated by Lagrange's equations. Finally, eq. (11) can be used to express this force in the articular space.

VIII. Control scheme

IX. Conclusion

This paper briefly presented the kinematic modelling of a kinematically redundant spatial parallel mechanism that is akin to the GS platform. This architecture, first introduced in [15], uses kinematic redundancy to avoid singularities and improve the workspace of the mechanism.

Jacobian matrices which include the redundant dofs as Cartesian dofs are presented in this paper. These matrices can be used for a numerical direct kinematic resolution. The inverse kinematics is shown to be very simple when the redundant dofs are included in an extended Cartesian velocity vector.

An algorithm for solving the direct kinematics is given. A force transmission index is introduced and is used to evaluate the performance of the robot. A static model is introduced in order to compensate for gravity during the control of the mechanism. Finally, a control scheme for physical human-robot interaction is introduced.

Acknowledgment

This work was supported by the Natural Sciences and Engineering Research Council of Canada (NSERC), and by the Canada Research Chair program.

References

[1] S. Advani, M. Nahon, N. Haeck, and J. Albronda, "Optimization of six-degrees-of-freedom motion systems for flight simulators," *Journal of Aircraft*, vol. 36, no. 5, pp. 819–826, 1999.

[2] L.-C. Lin and M.-U. Tsay, "Modeling and control of micropositioning systems using stewart platforms," *Journal of Robotic Systems*, vol. 17, no. 1, pp. 17–52, 2000.

[3] F. Pierrot, C. Reynaud, and A. Fournier, "Delta: a simple and efficient parallel robot," *Robotica*, vol. 8, no. 2, pp. 105–109, 1990.

[4] K. H. Pittens and R. P. Podhorodeski, "A family of stewart platforms with optimal dexterity," *Journal of Robotic Systems*, vol. 10, no. 4, pp. 463–479, 1993.

[5] K. E. Zanganeh and J. Angeles, "Kinematic isotropy and the optimum design of parallel manipulators," *The International Journal of Robotics Research*, vol. 16, no. 2, pp. 185–197, 1997.

[6] Y. Yun and Y. Li, "Design and analysis of a novel 6-dof redundant actuated parallel robot with compliant hinges for high precision positioning," *Nonlinear Dynamics*, vol. 61, no. 4, pp. 829–845, 2010.

[7] J.-P. Merlet, "Redundant parallel manipulators," *Laboratory Robotics and Automation*, vol. 8, no. 1, pp. 17–24, 1996.

[8] C. Gosselin and J. Angeles, "Singularity analysis of closed-loop kinematic chains," *IEEE Transactions on Robotics and Automation*, vol. 6, no. 3, pp. 281–290, 1990.

[9] J.-P. Merlet, "Singular configurations of parallel manipulators and Grassmann geometry," *The International Journal of Robotics Research*, vol. 8, no. 5, pp. 45–56, 1989.

[10] I. Bonev, "The true origins of parallel robots," Jan. 2003, uRL: http://www. parallemic, org/Reviews/Review007, html, 2007. 08.12.

[11] V. Gough and S. Whitehall, "Universal tyre test machine," in *Proc. FISITA 9th Int. Technical Congress*, 1962, pp. 117–137.

[12] C. Gosselin and L.-T. Schreiber, "Redundancy in parallel mechanisms: A review," *Applied Mechanics Reviews*, vol. 70, no. 1, p. 010802, 2018.

[13] C. Gosselin, T. Laliberté, and A. Veillette, "Singularity-free kinematically redundant planar parallel mechanisms with unlimited rotational capability," *IEEE Transactions on Robotics*, vol. 31, no. 2, pp. 457–467, 2015.

[14] L.-T. Schreiber and C. Gosselin, "Kinematically redundant planar parallel mechanisms: Kinematics, workspace and trajectory planning," *Mechanism and Machine Theory*, vol. 119, pp. 91–105, 2017.

[15] C. Gosselin and L.-T. Schreiber, "Kinematically redundant spatial parallel mechanisms for singularity avoidance and large orientational workspace," *IEEE Transactions on Robotics*, vol. 32, no. 2, pp. 286–300, 2016.

[16] J.-P. Merlet, *Parallel robots*, 2nd ed., G. Gladwell, Ed. The Netherlands: Springer, 2006, vol. 128.

[17] S. Chiaverini, "Singularity-robust task-priority redundancy resolution for real-time kinematic control of robot manipulators," *IEEE Transactions on Robotics and Automation*, vol. 13, no. 3, pp. 398–410, 1997.

[18] Y. Nakamura, H. Hanafusa, and T. Yoshikawa, "Task-priority based redundancy control of robot manipulators," *The International Journal of Robotics Research*, vol. 6, no. 2, pp. 3–15, 1987. [Online]. Available: http://ijr.sagepub.com/content/6/2/3.abstract

[19] M. Tandirci, J. Angeles, and F. Ranjbaran, "The characteristic point and the characteristic length of robotic manipulators," in *Proceedings of ASME 22nd Biennial Conference Robotics, Spatial Mechanisms and Mechanical System, Scotsdale, AZ*, vol. 45, 1992, pp. 203–208.

[20] C.-C. Lin and W.-T. Chang, "The force transmissivity index of planar linkage mechanisms," *Mechanism and Machine Theory*, vol. 37, no. 12, pp. 1465–1485, 2002.

[21] G. Sutherland and B. Roth, "A transmission index for spatial mechanisms," *Journal of Engineering for Industry*, vol. 95, no. 2, pp. 589–597, 1973.

[22] P. Cardou, S. Bouchard, and C. Gosselin, "Kinematic-sensitivity indices for dimensionally nonhomogeneous Jacobian matrices," *Robotics, IEEE Transactions on*, vol. 26, no. 1, pp. 166–173, 2010.